

RESEARCH ARTICLE

ASC Induces Apoptosis via Activation of Caspase-9 by Enhancing Gap Junction-Mediated Intercellular Communication

Masato Kitazawa^{1,2*}, Shigeaki Hida³, Chifumi Fujii², Shun'ichiro Taniguchi², Kensuke Ito², Tomio Matsumura², Nagisa Okada², Takashi Sakaizawa¹, Akira Kobayashi¹, Michiko Takeoka¹, Shin-ichi Miyagawa¹

1 Department of Surgery, Shinshu University School of Medicine, Matsumoto, Japan, **2** Department of Molecular Oncology, Shinshu University Graduate School of Medicine, Matsumoto, Japan, **3** Department of Molecular and Cellular Health Science, Nagoya City University Graduate School of Pharmaceutical Sciences, Mizuho-ku, Nagoya, Japan

* kita118@shinshu-u.ac.jp



OPEN ACCESS

Citation: Kitazawa M, Hida S, Fujii C, Taniguchi S, Ito K, Matsumura T, et al. (2017) ASC Induces Apoptosis via Activation of Caspase-9 by Enhancing Gap Junction-Mediated Intercellular Communication. PLoS ONE 12(1): e0169340. doi:10.1371/journal.pone.0169340

Editor: Aamir Ahmad, University of South Alabama Mitchell Cancer Institute, UNITED STATES

Received: June 16, 2016

Accepted: December 15, 2016

Published: January 5, 2017

Copyright: © 2017 Kitazawa et al. This is an open access article distributed under the terms of the [Creative Commons Attribution License](https://creativecommons.org/licenses/by/4.0/), which permits unrestricted use, distribution, and reproduction in any medium, provided the original author and source are credited.

Data Availability Statement: All relevant data are within the paper.

Funding: This work was funded by a grant No 20012020 from the Ministry of Education, Culture, Sport, Science and Technology, Japan. The funders had no role in study design, data collection and analysis, decision to publish, or preparation of the manuscript.

Competing Interests: The authors have declared that no competing interests exist.

Abstract

ASC (apoptosis-associated speck-like protein containing a CARD) is a key adaptor molecule of inflammasomes that mediates inflammatory and apoptotic signals. Aberrant methylation-induced silencing of ASC has been observed in a variety of cancer cells, thus implicating ASC in tumor suppression, although this role remains incompletely defined especially in the context of closely neighboring cell proliferation. As ASC has been confirmed to be silenced by abnormal methylation in HT1080 fibrosarcoma cells as well, this cell line was investigated to characterize the precise role and mechanism of ASC in tumor progression. The effects of ASC were examined using *in vitro* cell cultures based on comparisons between low and high cell density conditions as well as in a xenograft murine model. ASC overexpression was established by insertion of the ASC gene into pcDNA3 and pMX-IRES-GFP vectors, the latter being packed into a retrovirus and subjected to reproducible competitive assays using parental cells as an internal control, for evaluation of cell viability. p21 and p53 were silenced using shRNA. Cell viability was suppressed in ASC-expressing transfectants as compared with control cells at high cell density conditions in *in vitro* culture and colony formation assays and in *in vivo* ectopic tumor formation trials. This suppression was not detected in low cell density conditions. Furthermore, remarkable progression of apoptosis was observed in ASC-introduced cells at a high cell density, but not at a low one. ASC-dependent apoptosis was mediated not by p21, p53, or caspase-1, but rather by cleavage of caspase-9 as well as by suppression of the NF-κB-related X-linked inhibitor-of-apoptosis protein. Caspase-9 cleavage was observed to be dependent on gap junction formation. The remarkable effect of ASC on the induction of apoptosis through caspase-9 and gap junctions revealed in this study may lead to promising new approaches in anticancer therapy.

Introduction

Containing 2 death domains, caspase recruitment domains (CARD) and pyrin domains [1], the ASC protein has been shown to form aggregates in human myelocytic leukemia HL-60 cells undergoing apoptosis [2]. ASC has also been established as a key adaptor molecule of inflammasomes, activating the procaspase-1 that is necessary for processing IL-1 β [3] and IL-18 [4]. Inflammasomes are critical for host defense; dysregulation of their activation contributes not only to pathogenic inflammation, but also to chronic inflammatory diseases, such as metabolic syndrome [5] and age-related disease [6]. Furthermore, inflammasome- or caspase-1-deficient mice exhibited increased tumor formation [7], and inflammasome- and IL-1 β -dependent chronic inflammation contributed to the initiation and progression of cancer [8].

The ASC gene is known to be downregulated in human breast cancer as a result of the aberrant hyper-methylation of DNA in its promoter CpG islands [9, 10], which has since been documented in various cancers. In our previous study, silenced ASC was re-expressed by treatment with the DNA methyltransferase inhibitor 5'-aza-2'-deoxycytidine (5'-aza-dC) in methylation-positive human melanoma [11] and colorectal cancer [12] cell lines. This epigenetic inhibition of ASC in cancer cells implied a possible role as a tumor suppressor gene [13].

Thereafter, numerous studies have demonstrated an inhibitory effect of ASC on tumorigenesis. Colorectal cancer was enhanced upon genetic deletion of caspase-1 or ASC [14], while ASC-overexpressing lymphoma cells showed reduced metastasis [15]. The understanding of the mechanisms of ASC has progressed as well, with reports of tumorigenesis inhibition in primary melanoma via ASC expression by restricting NF- κ B activity [16] and decreased P53- and p21-related cell apoptosis by knockdown of ASC [17].

Intercellular communication halts normal cell proliferation by cell cycle arrest when cells reach a high density in culture conditions. However, this cell contact inhibition is frequently impaired in tumor cells, resulting in abnormal proliferation [18]. Several signaling pathways, including those of p53 [19], p21 [20], cadherin [21], and mTOR and p27 [22], have been studied to address this phenomenon. The present study turned to the role of ASC in this aberrant viability at a high cell density with a focus on apoptosis and gap junctions, i.e., intercellular communication-dependent programmed cell death, in the HT1080 malignant phenotype human fibrosarcoma cell line. Gap junctions provide a direct route for metabolites and signaling molecules to pass from cell to cell. As decreased expression of gap junction-related molecules inhibited intercellular communication in many cancer cell lines [23, 24], dysregulation of junctional communication might play a critical role of cancer development.

The ASC-dependent apoptosis was elicited by the activation of caspase-9 and suppression of NF- κ B-related X-linked inhibitor-of-apoptosis protein (XIAP) in a gap junction-mediated fashion. Moreover, reproducible competitive assays using FACS analysis based on internal controls were established for the precise evaluation of cell viability.

Materials and Methods

Cell culture

Cells from the HT1080 Human fibrosarcoma cell line, HT1080, was obtained from the IFO Animal Cell Bank (Osaka, Japan) and cultured in Dulbecco's modified Eagle's medium supplemented with 10% fetal bovine serum at 37°C in 5% CO₂.

Quantitative reverse-transcription polymerase chain reaction (RT-PCR)

Total RNA was extracted with NucleoSpin RNAII (Takara Bio, Otsu, Japan), and RT was performed with PrimeScript[®] RT Master Mix (Takara Bio). The PCR was set up with SYBER

Table 1. Primer sequences used for quantitative RT-PCR.

Gene name	Primer sequence (5'-3')
β-actin	F: GGACTTCGAGCAAGAGATGG
	R: GTGGATGCCACAGGACTCCAT
ASC	F: CTCCTCAGTCGGCAGCCAAG
	R: ACAGAGCATCCAGCAGCCAC
p53	F: TTCGACATAGTGTGGTGGTGC
	R: GCCCATGCAGGAAGTGTACAC
p21	F: AGGTGGACCTGGAGACTCTCAG
	R: GCTTCTCTTGGAGAAGATCAGC
IL-1β	F: ACAGATGAAGTGCTCCTTCCA
	R: GTCGGAGATTCTAGCTGGAT
MMP-9	F: TGACGAGTTGTGGTCCCTGG
	R: AGGAGCGGCCCTCGAAGATGAAG
VEGF	F: CGAAACCATGAACCTTCTGC
	R: CCTCAGTGGGCACACTCC
XIAP	F: TGGTTGCAGATCTAGTGAATGCTC
	R: CGCCTTAGCTGCTCTTTCAGTAC
Connexin 43	F: TTCATGCTGGTGGTGCCTTG
	R: GCTCTTCCCTTAACCCGATCC

doi:10.1371/journal.pone.0169340.t001

Premix Ex Taq™ II (Takara Bio) and carried out on a Thermal Cycler Dice Real Time System II device (Takara Bio). The sequences of the specifically designed primers are listed in [Table 1](#).

Western blotting analysis

Cells were lysed in lysis buffer containing 20 mM Tris-HCl pH 7.5, 150 mM NaCl, 0.5% deoxycholic acid, 1% NP-40, 2 mM EDTA, 1% SDS, 1 mM phenylmethyl sulfonyl fluoride, 1 mM sodium orthovanadate, 25 mM NaF, and 1x complete protease inhibitor cocktail (Roche, Mannheim, Germany) for 30 minutes at 4°C. The lysates were separated by 15% SDS-PAGE. The anti-human ASC mAb described previously ([2]; MBL, Nagoya, Japan) and anti-human caspase-9 mAb (Cell Signaling Technology, Beverly, MA) were adopted in Western blotting assays.

Transfection of plasmid vectors and establishment of stable clones

Human full-length ASC genes were inserted into pcDNA3 vectors (Invitrogen, Carlsbad, CA). Empty pcDNA3 vectors (control) and ASC/pcDNA3 vectors (ASC) were transduced into HT1080 cells with GeneJuice (Novogen, San Diego, CA). G418-resistant clones were selected at 14 days of incubation.

Cell viability and colony formation assays

For *in vitro* viability assays, 3×10^4 of control or ASC-expressing cells were seeded onto 60 mm plates for low cell density culture conditions or onto 12-well plates for high cell density culture conditions. In colony formation assays, approximately 500 cells were seeded onto 100 mm plates and incubated for 11 days. Colonies larger than 0.25 mm^2 were counted using NIH Image J software.

Tumorigenesis *in vivo*

To examine tumorigenesis *in vivo*, 1×10^6 of control or ASC-expressing cells were subcutaneously injected into the flanks of 7-week-old male BALB/c nude mice (CLEA Japan, Tokyo, Japan). Tumor volume was evaluated using the formula of: volume (mm^3) = $0.5 \times \text{width}^2$ (mm) \times length (mm). All mice were sacrificed by means of sodium pentobarbital anesthesia on day 12. Experiments were carried out in accordance with the Guidelines for Animal Care and Experimentation of Shinshu University School of Medicine.

TUNEL and immunohistochemistry

In situ detection of DNA fragmentation in tumor tissues was performed using TUNEL staining with *in situ* apoptosis detection kits (Takara Bio). For the staining of Ki-67 (mAb, DAKO, Kyoto, Japan), antigen retrieval was done by boiling sections in a microwave oven in 0.01 M citric acid, pH 6.0. The numbers of TUNEL- and Ki-67-positive cells were counted in random high-power fields.

Retroviral transduction

For retroviral transduction, the ASC gene was inserted into pMX-IRES-GFP vectors (Cell Biolab, Inc., San Diego, CA), which were then transfected into amphotropic packaging cells using GeneJuice (Novogen). The virus-containing supernatants were harvested at 24 h and 48 h. Retrovirus infection was performed on RetroNectin (Takara Bio)-coated plates. Transduction efficiency was confirmed in terms of GFP-positive ratio by flow cytometry (FACS, BD FACS Canto II, Becton Dickinson, Franklin Lakes, NJ), and the early-passaged cells were used in subsequent experiments.

Competitive assays

Competitive assays were conducted using parental cells as an internal control for enhanced objectivity and reproducibility. After retroviral transduction with pMX-IRES-GFP vectors, vector-transduced HT1080 cells (GFP-positive) and non-treated parental cells (GFP-negative) were mixed at approximately equal amounts. For low cell density assays, 3×10^4 of mixed cells were seeded onto 12-well plates on day 0, i.e., 1.5×10^4 of parental cells and 1.5×10^4 of pMX-IRES-GFP vector-transfected cells (control) or 1.5×10^4 of pMX-IRES-GFP/ASC vector-transfected cells (ASC-expressing). For high cell density assays, 3×10^5 of mixed cells were seeded onto 12-well plates in an identical fashion. The ratio of GFP-positive cells to parental cells was determined by FACS and defined as “GFP-positive cell ratio”. Then, “relative GFP-positive ratio (%)” was calculated as: $100 \times (\text{GFP-positive cell ratio on target day} / \text{GFP-positive cell ratio on day 0})$.

Annexin V and 7-AAD staining

For evaluation of cell death, cells were harvested and resuspended in Annexin V Binding Buffer (BioLegend, San Diego, CA) followed by Alexa Fluor 647-conjugated annexin V (BioLegend) for 15 min at room temperature. Cells were further resuspended in Annexin V Binding Buffer dissolved with 7-AAD (BioLegend). The double-positive percentage of annexin V and 7-AAD was analyzed by FACS.

Knockdown of p53, p21 and connexin 43

For knockdown of the retroviral-mediated target genes p53, p21, and connexin 43, shRNA sequences were ligated into pSINsi-hU6 or pSINsi-DK I vectors (Takara Bio) as listed in

Table 2. Target sequences for shRNA.

Target gene	Vector	Promoter	Targeted sequence (5'-3')
Scramble	pSINsi-hU6	U6	TCTTAATCGCGTATAAGGC
p53	pSINsi-hU6	U6	GACTCCAGTGGTAATCTAC
p21	pSINsi-hU6	U6	TCACTGTCTTGTACCCTTGT
Connexin 43	pSINsi-DK I	U6	Cx43DNA1: TGAGTACCACCTCCACCGG
			Cx43DNA2: TAAATACCAACATGCACCT

doi:10.1371/journal.pone.0169340.t002

Table 2. G418-resistant cells were selected at 14 days of incubation. Knockdown efficiencies were confirmed by quantitative RT-PCR analysis.

Statistical analysis

Statistical significance was evaluated using the Student's *t*-test on the data of 3–8 experiments for each assay. A *p* value of <0.05 was accepted as statistically significant. All values were expressed as the mean ± standard error of the mean.

Results

ASC suppressed cell viability in high, but not low, cell density conditions

As the expression of ASC was found to be decreased in several progressive cancer cell lines by aberrant methylation, we treated HT1080 cells with the demethylating reagent 8μM 5'-aza-dC (Sigma-Aldrich, St. Louis, MO) and observed that demethylation increased the expression of ASC mRNA by 12.8-fold (Fig 1A) in addition to ASC protein level (Fig 1B) in repeated experiments, indicating that the ASC gene was indeed silenced by methylation in HT1080 cells. Thereafter, we established stably transfected HT1080 clones expressing ASC for investigation of the effects of ASC on cell viability and colony-forming activity *in vitro*. The expression of transfected ASC introduced into pcDNA3 vectors was confirmed by Western blotting (Fig 1C).

When cells were plated at a low cell density, the viability rate was similar between ASC-expressing and control vector-transfected cells (Fig 1D). In contrast, the viability of ASC-expressing cells was significantly suppressed on day 8 as compared with control cells in a high density culture (Fig 1E). Furthermore, the number of colonies, which mimicked the *in vivo* environment, was significantly smaller for ASC-expressing cells (Fig 1F). These results indicated that ASC suppressed cell viability at a high cell density, presumably through close interactions with neighboring cells, but not at a low density.

ASC negatively regulated tumorigenesis *in vivo*

We next examined the effects of ASC on tumorigenicity *in vivo*. As shown in Fig 2A, the tumor volume of ASC-expressing cells was significantly smaller than that of control cells on day 12. Tumor weight was also significantly lower in ASC-expressing cells (Fig 2B). The number of TUNEL-positive apoptotic cells in ASC-transfected tumors was increased by 4-fold as compared with that of control tumors (Fig 2C), while no significant differences were observed for Ki-67 expression (Fig 2D). These results suggested that ASC regulated tumor formation by the induction of apoptosis rather than by cell cycle retardation.

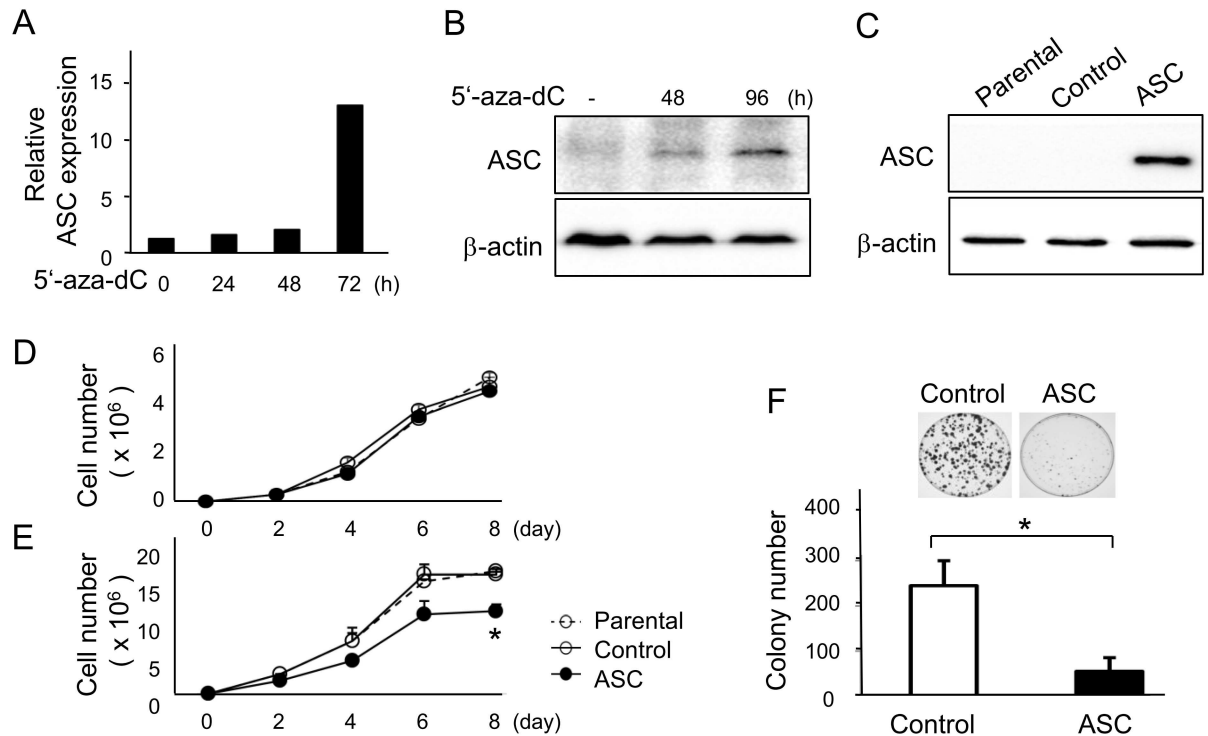


Fig 1. 5'-aza-dC treatment restored ASC expression and overexpression of ASC suppressed cell viability in high cell density cultures. HT 1080 cells were treated with 8μM 5'-aza-dC, and expression of ASC was detected by (A) quantitative RT-PCR (n = 2) and (B) Western blotting. (C) Expression of ASC inserted into pcDNA3 vectors and stably transfected into cells was confirmed by Western blotting. Viability of ASC-expressing and control cells at (D) a low cell density (n = 8), (E) a high cell density (n = 8), and (F) in colony formation assays (n = 3). *p<0.05.

doi:10.1371/journal.pone.0169340.g001

Confirmation of the suppressive effect of ASC on cell viability by competitive assays

Retrovirus-expressing bicistronic message-encoding ASC and GFP were prepared for competitive assays. ASC transduction was detected by Western blot analysis (Fig 3A), and a positive correlation ASC with GFP was confirmed by FACS analysis (Fig 3B). The cells were transfected with greater than 90% efficiency by the retroviral vector. GFP-transduced cells did not exhibit markedly altered growth kinetics or GFP-positive cell ratio.

The GFP-positive cell ratio was expected to decrease in ASC-expressing cells via an inhibitory effect on viability. This was evident by FACS on day 14 in high cell density cultures, indicating that ASC suppressed cell viability (Fig 3C). The relative GFP-positive ratio was significantly decreased in ASC-expressing cells as compared with control cells at a high cell density as well (Fig 3D). Such findings confirmed that the competitive mix culture was a reproducible and reliable method for the evaluation of cell viability, which was therefore employed for subsequent experiments. Here, GFP-positive cell ratio was the ratio of GFP-positive cells to parental cells, after which relative GFP-positive ratio (%) was calculated as: 100 x (GFP-positive cell ratio on target day / GFP-positive cell ratio on day 0), as described in the Materials and Methods.

ASC-mediated apoptosis, but not necrosis, was induced in high cell density conditions

ASC suppressed relative GFP-positive ratio more readily at a high cell density as compared with at a low cell density (Fig 4A and 4B). The status of apoptosis was examined with annexin

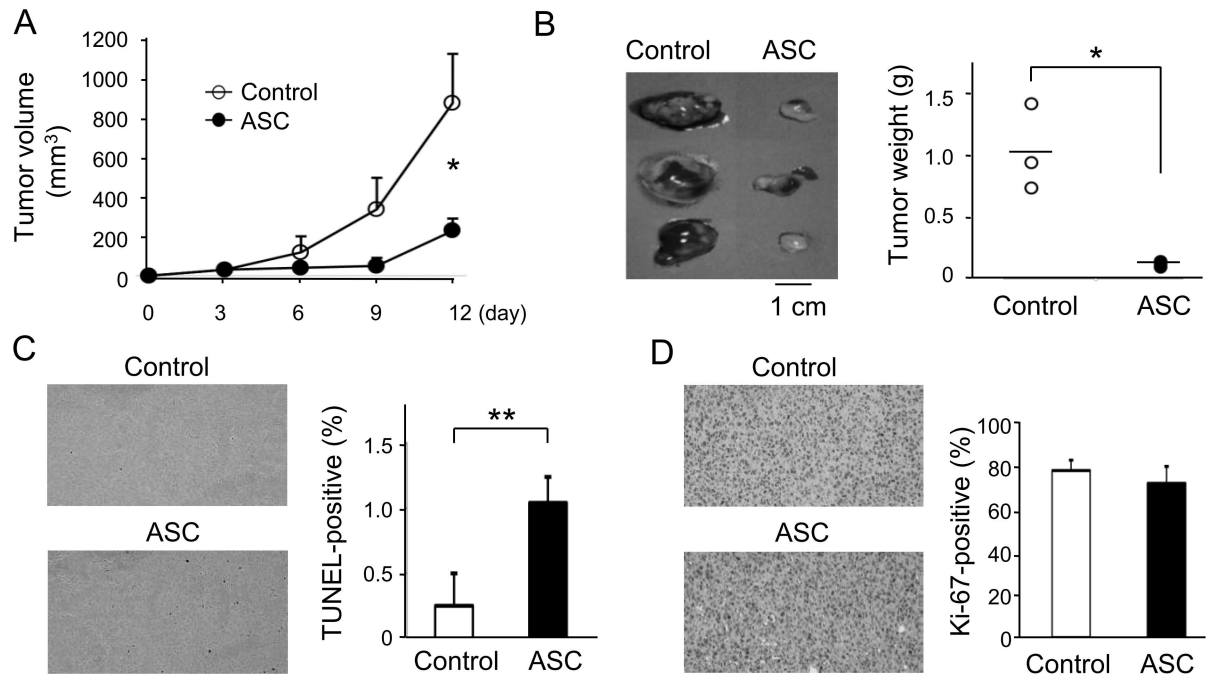


Fig 2. ASC negatively regulated tumorigenesis *in vivo*. (A) Tumor volumes of ASC-expressing and control cells subcutaneously inoculated into the flanks of immunodeficient mice (n = 3). (B) Tumor weights of mice sacrificed on day 12. Staining and number of (C) TUNEL-positive apoptotic cells (n = 6) and (D) Ki-67-positive cells (n = 6). *p<0.05, **p<0.01.

doi:10.1371/journal.pone.0169340.g002

V/7-AAD using FACS at 4 days after inoculation. At a low cell density, the cell populations undergoing apoptosis were minimal, and there was no significant difference between ASC-expressing and control cells (Fig 4C). On the other hand, at a high cell density, ASC-expressing cells had significant, 3-fold increased percentages of annexin V/7-AAD double-positive cells, i.e., late apoptosis or necrotic cells, as compared with control cells (Fig 4C).

We next sought to distinguish the precise factor causing cell death as either apoptosis or necrosis. An inhibitor of RIP-1-dependent necrosis (Necrostatin-1, BioMol, Plymouth

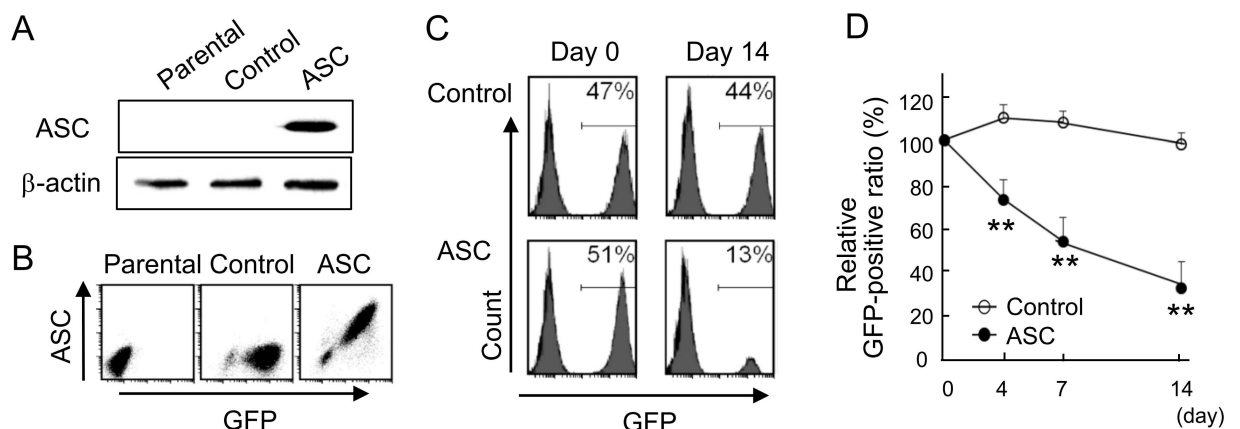


Fig 3. Competitive assays using retroviruses containing vectors bicentrically encoded with GFP and ASC. (A) Expression of ASC inserted into pMX-IRES-GFP vectors was confirmed by Western blotting. (B) A correlation of ASC with GFP was disclosed by FACS. (C) Population of GFP-positive cells simultaneously expressing ASC on day 14 as detected by FACS. (D) Time course of relative GFP-positive ratio in a high cell density culture (n = 4). **p<0.01.

doi:10.1371/journal.pone.0169340.g003

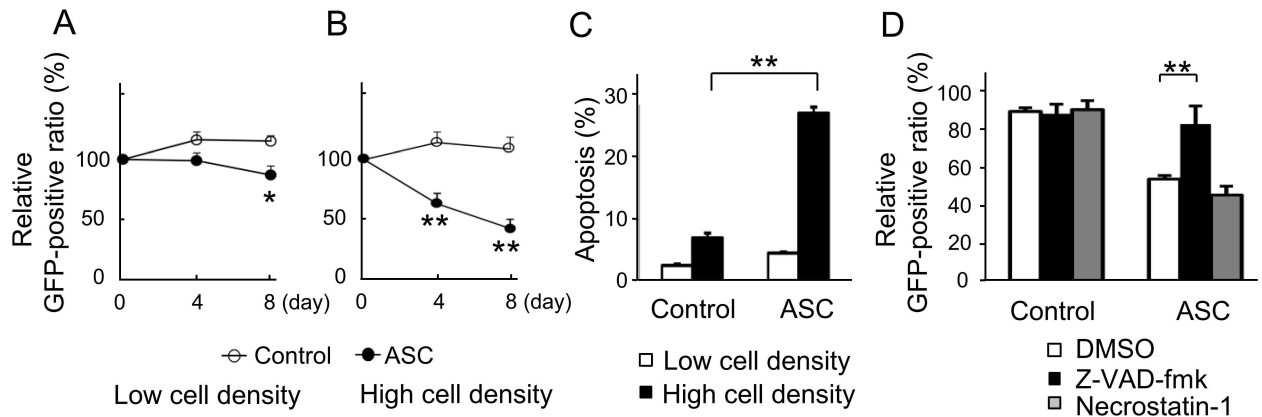


Fig 4. ASC-mediated apoptosis, but not necrosis, was induced in high cell density conditions. Comparison of relative GFP-positive ratio between control and ASC-expressing cells at (A) a low cell density and (B) a high cell density (n = 6 for each). (C) Percentage of annexin V/7-AAD double-positive cells as detected by FACS. (D) Treatment of cells with a pan-apoptosis inhibitor (Z-VAD-fmk) or inhibitor of necrosis (Necrostatin-1) at a high cell density (n = 4). *p<0.05, **p<0.01.

doi:10.1371/journal.pone.0169340.g004

Meeting, PA) failed to abrogate ASC-dependent cell death, whereas a pan-caspase inhibitor (Z-VAD-fmk, MBL) almost completely blocked ASC-dependent cell death (Fig 4D). These results indicated that the reduced number of ASC-expressing cells was associated with an increase in apoptosis, and not necrosis, which was consistent with our *in vivo* experiments.

ASC-mediated apoptosis induced at a high cell density was independent of p53 and p21 function

To determine if p53 or p21 function was required for ASC-induced apoptosis at a high cell density, we generated p53- or p21-silenced HT1080 cells by retroviral shRNA-mediated knockdown that was confirmed by quantitative RT-PCR (Fig 5A and 5B). Unexpectedly, knockdown of neither p53 nor p21 attenuated ASC-dependent apoptosis in viability assays (Fig 5C), indicating that the apoptosis induced by ASC at a high cell density occurred in a p53- and p21-independent manner.

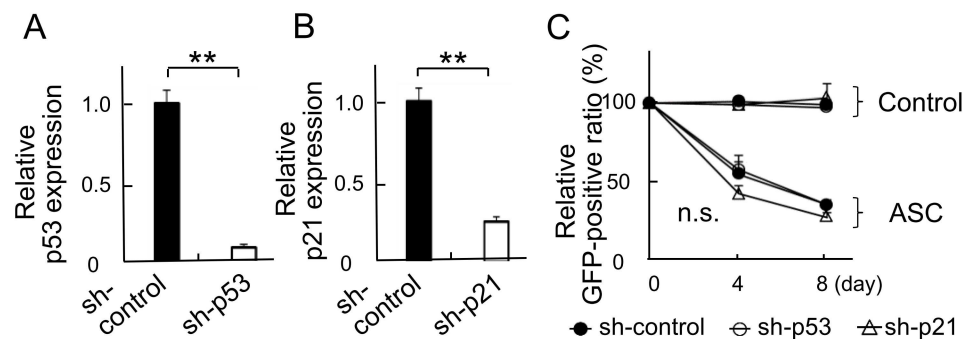


Fig 5. Knockdown of p53 or p21 with shRNA did not affect ASC-dependent apoptosis at a high cell density. Expression of (A) p53 and (B) p21 was confirmed by quantitative RT-PCR (n = 6 for each). (C) Effect of p53 or p21 knockdown on control and ASC-expressing cell relative GFP-positive ratio (n = 6 for each). **p<0.01, n.s.: not significant.

doi:10.1371/journal.pone.0169340.g005

Gap junction-mediated activation of caspase-9 promoted ASC-dependent apoptosis at a high cell density

Since NF- κ B has been shown to correlate with ASC and apoptosis, the involvement of NF- κ B-related molecules was investigated to elucidate the pathway of the ASC-dependent apoptosis caused in high cell density conditions. Quantitative RT-PCR analysis demonstrated that the expressions of the NF- κ B-related genes *IL-1 β* and *XIAP* were significantly suppressed in ASC-expressing cells as compared with controls at a high cell density (Fig 6A). No such difference was observed at a low cell density. The induction of ASC has been documented to activate caspase-1 and process pro IL-1 β [25], while XIAP was reported to inhibit the activation of caspase-9 [26]. Therefore, caspase-1 and caspase-9 were judged to be candidates involved in the ASC-dependent apoptosis in high cell density conditions.

A pan-caspase inhibitor (Z-VAD-fmk, MBL) blocked ASC-dependent cell death. An inhibitor of caspase-9 (Z-LEHD-fmk, MBL) significantly abrogated ASC-dependent cell death as well, but a caspase-1 inhibitor (Z-YVAD-fmk, MBL) did not produce any marked alterations (Fig 6B). These results indicated that the ASC-facilitated apoptosis was at least partially mediated by caspase-9. We subsequently analyzed the potential activation of endogenous caspase-9 in response to ASC induction. The protein level of cleaved caspase-9 in ASC-expressing cells was remarkably higher than that in controls at a high cell density, but not at a low one; caspase-9 cleavage was hardly detectable in low cell density conditions (Fig 6C).

Lastly, since the loss of gap junction-mediated intercellular communication has been shown to facilitate tumorigenesis and tumor cell survival, we investigated the expression of connexin involved in gap junction assembly. The mRNA expression of connexin 43 was slightly increased at a high density in control cells, while significantly increased connexin 43 mRNA expression was observed in ASC-expressing cells at a high density (Fig 6D). We further analyzed the role of gap junctions in ASC-dependent apoptosis via the evaluation of caspase-9 cleavage. The gap junction inhibitor carbenoxolone (CBX; Sigma-Aldrich) significantly attenuated the growth inhibitory effects of ASC (Fig 6E) and the cleavage of caspase-9 in ASC-expressing cells (Fig 6F). As CBX was not specific for gap junctions, we also performed knock-down of connexin 43 to disassemble gap junctions. Connexin 43 was confirmed to be effectively silenced (Fig 6G). Cleaved caspase-9 was observed in ASC-expressing cells at a high cell density, which was prevented in ASC-expressing, connexin 43-silenced cells. These results inferred that suppression of cell growth by ASC at a high density at least partially depended on gap junctional communication.

Discussion

After observing that the viability of HT1080 fibrosarcoma cells was suppressed by ASC when in close proximity to neighboring cells, we examined several signaling pathways to reveal that ASC suppressed XIAP expression, enhanced the involvement of gap junctions, and consequently activated caspase-9, which resulted in the induction of apoptosis, and not necrosis, in HT1080 fibrosarcoma cells via close interactions with adjacent cells in high density conditions.

In the murine *in vivo* experiment, the suppression of tumorigenesis by ASC induction was suggested to occur by apoptosis rather than cell cycle arrest. Therefore, we focused on programmed cell death and investigated its characteristics in *in vitro* experiments based on comparisons between low and high cell density conditions. ASC-expressing cells exhibited increased apoptosis at a high cell density. ASC has been reported to play an essential role in the intrinsic mitochondrial pathway of apoptosis through a p53-Bax network [27], with the anti-tumorigenic function of ASC being partially regulated by the activation of p53 and p21

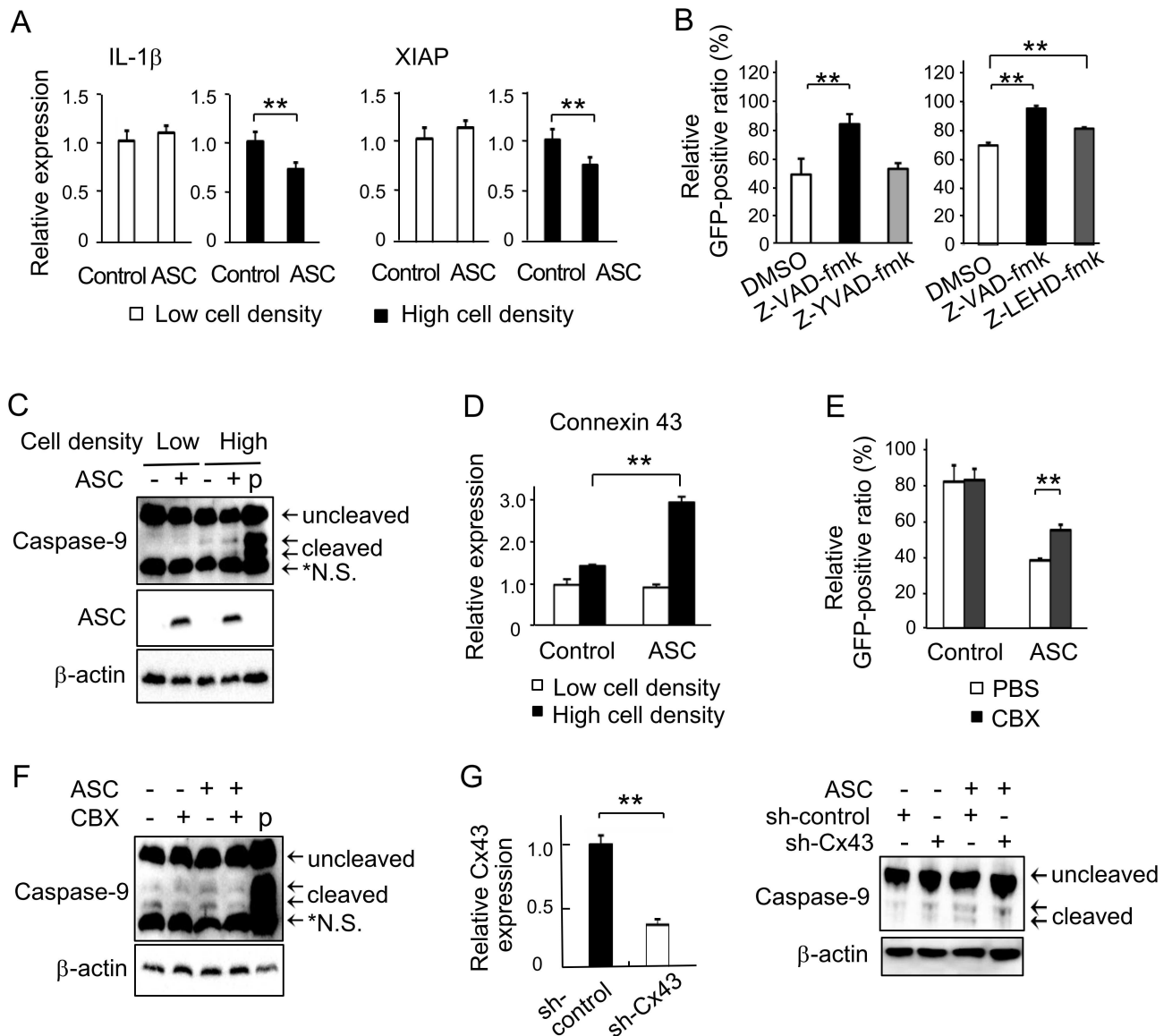


Fig 6. Involvement of caspase-9 and gap junctions on ASC-dependent apoptosis at a high cell density. (A) Relative mRNA expressions of the NF-κB-regulated genes IL-1β and XIAP were evaluated by quantitative RT-PCR at both low and high cell densities (n = 4 for each). (B) Effects of caspase inhibitors on ASC-dependent apoptosis as evaluated by relative GFP-positive ratio at a high cell density. Z-VAD-fmk; pan-caspase inhibitor, z-YVAD-fmk; caspase-1 inhibitor, Z-LEHD-fmk; caspase-9 inhibitor (n = 4 for each). (C) Activation of caspase-9 induced by ASC introduction as detected by Western blotting at low and high cell densities. (D) Relative mRNA expression of connexin 43 evaluated by quantitative RT-PCR at both low and high cell densities (n = 3 for each). (E) Effect of the gap junction inhibitor CBX on relative GFP-positive ratio at a high cell density (n = 4). (F) Effects of CBX on the activation of caspase-9 at a high cell density by Western blotting. (G) Confirmation of connexin 43 (Cx 43) silencing performed by quantitative RT-PCR (n = 3). And effects of connexin 43 silencing on the activation of caspase-9 at high cell density by Western blotting. Representative results of triplicate experiments. **p<0.01.

doi:10.1371/journal.pone.0169340.g006

signaling [17]. However, experiments with shRNA revealed that the ASC-dependent apoptosis induced at a high cell density in this study was independent of p53 and p21.

Erl et al. described that NF-κB inhibition increased cell death at a low cell density, while cells in high density cultures exhibited high NF-κB activity and were insensitive to the induction of apoptosis [28]. Forced expression of ASC was seen to enhance NF-κB activity in metastatic melanoma but inhibit NF-κB in primary melanoma [16], indicating that the effects of

ASC on NF- κ B depended on the degree of malignancy and cellular context. Based on these studies, we investigated the effects of ASC on several NF- κ B-related genes and witnessed that ASC inhibited the induction of the NF- κ B-dependent genes IL-1 β and XIAP at a high cell density. IL-1 β is a major target of caspase-1 and XIAP has been reported to regulate the activity of caspase-9 and inhibit apoptosis [29]. Here, trials with z-YVAD-fmk, an inhibitor of caspase-1, and z-LEHD-fmk, an inhibitor of caspase-9, revealed that ASC-dependent apoptosis in high cell density conditions was likely mediated by the cleavage of caspase-9 only.

ASC has been reported to trigger Fas ligand-induced caspase-8-dependent apoptosis [30, 31], but reports on ASC and caspase-9 are few. McConnell et al. [32] demonstrated that ASC (TMS1)-induced apoptosis proceeded through a CARD-dependent aggregation step followed by the activation of a caspase-9-mediated pathway. In general, death-inducing signaling complexes have been identified as activators of caspase-8 [33, 34], while apoptosomes provide the activation platform for initiation of caspase-9 [29, 35]. A recent study [36] revealed that caspase-9 was activated allosterically by binding to apoptosomes, in which a platform was assembled in response to mitochondria-dependent apoptosis under the influence of XIAP. In the inflammatory response, spinal cord injury activates inflammasomes containing ASC and leads to the cleavage of XIAP [37]. However, reports on this phenomenon are scarce, with even fewer related to tumors. It was intriguing that ASC activated caspase-9 with suppression of XIAP and resulted in apoptosis in a high cell density culture only.

We ensuingly addressed how increased cell density could possibly trigger caspase-9-activated apoptosis. Apoptosis was found to be induced at a high cell density in relation to TGF- β and Bcl-2 in HL-60 cells [37]. Cell-cell contact promoted the nuclear translocation of p21/Waf-1-induced cellular growth arrest and increased apoptosis [38]. Elsewhere, p53 activation was suppressed in density-plated cells [19]. An involvement of p21 or p53 in ASC-dependent apoptosis at a high cell density was excluded earlier in our experiment.

Cells constitutively interact with each other, and cell-cell communication through gap junction formation plays an imperative role in tumor cell survival and death. The loss of gap junctions assembled by connexins was reported to facilitate tumorigenesis in prostate [23] and liver [24] cancers. Therefore, we inhibited gap junction establishment by CBX or connexin 43 knockdown to elucidate its functions in apoptosis. They reduced the cleavage of caspase-9 and growth suppression by ASC induction, indicating that gap junctions were possible mediators of ASC-dependent apoptosis in HT1080 tumor cells in high cell density conditions. However, findings in a single cell line may not always be extrapolated to other cell types. According to Larson et al. [39], connexin 43 mRNA levels were high in subconfluent conditions but decreased at confluency in normal endothelial cells. Slightly increased mRNA amounts were, however, observed in our control cells, the level of which became significantly increased in ASC-expressing cells at a high density. Gap junction assembly by connexin 43 was documented to propagate cell-killing signals initially generated by a single cell spontaneously initiating apoptosis to surrounding cells in a bladder carcinoma cell line [40]. Since the expression of connexin 43 is regulated by the PI3K/AKT/mTOR and Mnk1/2 pathways [41], the role of ASC in gap junction signaling that occurs at a high density needs to be clarified.

It is noteworthy that the present study employed competitive assays in addition to stable clone assays. Since parental cells were mixed as an internal control and the ratio of transfectants to parental cells was evaluated by FACS, the competitive assays were believed to be relatively more objective and reproducible than conventional set-ups. Competitive assays also avoid the risk of selecting champion clones that limits the reliability of stable clone assays.

In conclusion, the remarkable effects of ASC on the induction of apoptosis through caspase-9 activation and gap junctions may have important bearings in tumor suppression and represent a promising new target in anticancer therapy.

Author Contributions

Conceptualization: SH MT SM.

Data curation: AK MT.

Formal analysis: MK CF.

Funding acquisition: ST.

Investigation: MK CF KI TM NO TS.

Methodology: SH.

Project administration: SM.

Supervision: MT.

Writing – original draft: MT.

References

1. Park HH, Lo YC, Lin SC, Wang L, Yang JK, Wu H. The death domain superfamily in intracellular signaling of apoptosis and inflammation. *Annu Rev Immunol.* 2007; 25:561–86. doi: [10.1146/annurev.immunol.25.022106.141656](https://doi.org/10.1146/annurev.immunol.25.022106.141656) PMID: [17201679](https://pubmed.ncbi.nlm.nih.gov/17201679/)
2. Masumoto J, Taniguchi S, Ayukawa K, Sarvotham H, Kishino T, Niikawa N, et al. ASC, a novel 22-kDa protein, aggregates during apoptosis of human promyelocytic leukemia HL-60 cells. *J Biol Chem.* 1999; 274(48):33835–8. PMID: [10567338](https://pubmed.ncbi.nlm.nih.gov/10567338/)
3. Martinon F, Burns K, Tschopp J. The inflammasome: a molecular platform triggering activation of inflammatory caspases and processing of proIL-beta. *Mol Cell.* 2002; 10(2):417–26. PMID: [12191486](https://pubmed.ncbi.nlm.nih.gov/12191486/)
4. Dinarello CA. Interleukin-1 beta, interleukin-18, and the interleukin-1 beta converting enzyme. *Ann NY Acad Sci.* 1998; 29; 856:1–11. Review. PMID: [9917859](https://pubmed.ncbi.nlm.nih.gov/9917859/)
5. Murphy AJ, Kraakman MJ, Kammoun HL, Dragoljevic D, Lee MK, Lawlor KE, et al. IL-18 production from the NLRP1 inflammasome prevents obesity and metabolic syndrome. *Cell Metab.* 2016 Jan 12; 23(1):155–64. Epub 2015 Oct 22. doi: [10.1016/j.cmet.2015.09.024](https://doi.org/10.1016/j.cmet.2015.09.024) PMID: [26603191](https://pubmed.ncbi.nlm.nih.gov/26603191/)
6. Samstad EO, Niyonzima N, Nymo S, Aune MH, Ryan L, Bakke SS, et al. Cholesterol crystals induce complement-dependent inflammasome activation and cytokine release. *J Immunol.* 2014; 192(6):2837–45. Epub 2014 Feb 19. doi: [10.4049/jimmunol.1302484](https://doi.org/10.4049/jimmunol.1302484) PMID: [24554772](https://pubmed.ncbi.nlm.nih.gov/24554772/)
7. Hu B, Elinav E, Huber S, Booth CJ, Strowig T, Jin C, et al. Inflammation-induced tumorigenesis in the colon is regulated by caspase-1 and NLRC4. *Proc Natl Acad Sci U S A.* 2010; 107(50):21635–40. Epub 2010 Nov 30. doi: [10.1073/pnas.1016814108](https://doi.org/10.1073/pnas.1016814108) PMID: [21118981](https://pubmed.ncbi.nlm.nih.gov/21118981/)
8. Okamoto M, Liu W, Luo Y, Tanaka A, Cai X, Norris DA, et al. Constitutively active inflammasome in human melanoma cells mediating autoinflammation via caspase-1 processing and secretion of interleukin-1beta. *J Biol Chem.* 2010; 285(9):6477–88. Epub 2009 Dec 28. doi: [10.1074/jbc.M109.064907](https://doi.org/10.1074/jbc.M109.064907) PMID: [20038581](https://pubmed.ncbi.nlm.nih.gov/20038581/)
9. Conway KE, McConnell BB, Bowring CE, Donald CD, Warren ST, Vertino PM. TMS1, a novel proapoptotic caspase recruitment domain protein, is a target of methylation-induced gene silencing in human breast cancers. *Cancer Res.* 2000; 60(22):6236–42. PMID: [11103776](https://pubmed.ncbi.nlm.nih.gov/11103776/)
10. Levine JJ, Stimson-Crider KM, Vertino PM. Effects of methylation on expression of TMS1/ASC in human breast cancer cells. *Oncogene.* 2003; 22(22):3475–88. doi: [10.1038/sj.onc.1206430](https://doi.org/10.1038/sj.onc.1206430) PMID: [12776200](https://pubmed.ncbi.nlm.nih.gov/12776200/)
11. Guan X, Sagara J, Yokoyama T, Koganehira Y, Oguchi M, Saida T. ASC/TMS-1, a caspase-1 activating adaptor, is down-regulated by aberrant methylation in human melanoma. *Int J Cancer.* 2003; 107(2):202–8. doi: [10.1002/ijc.11376](https://doi.org/10.1002/ijc.11376) PMID: [12949795](https://pubmed.ncbi.nlm.nih.gov/12949795/)
12. Yokoyama T, Sagara J, Guan X, Masumoto J, Takeoka M, Komiyama Y, et al. Methylation of ASC/TMS1, a proapoptotic gene responsible for activating procaspase-1, in human colorectal cancer. *Cancer Lett.* 2003; 202(1):101–8. PMID: [14643031](https://pubmed.ncbi.nlm.nih.gov/14643031/)
13. McConnell BB, Vertino PM. TMS1/ASC: the cancer connection. *Apoptosis.* 2004; 5–18. Review. doi: [10.1023/B:APPT.0000012117.32430.0c](https://doi.org/10.1023/B:APPT.0000012117.32430.0c) PMID: [14739594](https://pubmed.ncbi.nlm.nih.gov/14739594/)

14. Allen IC, TeKippe EM, Woodford RM, Uronis JM, Holl EK, Rogers AB, et al. The NLRP3 inflammasome functions as a negative regulator of tumorigenesis during colitis-associated cancer. *J Exp Med*. 2010; 207(5):1045–56. Epub 2010 Apr 12. doi: [10.1084/jem.20100050](https://doi.org/10.1084/jem.20100050) PMID: [20385749](https://pubmed.ncbi.nlm.nih.gov/20385749/)
15. Zhang Y, Zhang J, Lin C, Wei W, Ren S, Zuo Y. Overexpression of apoptosis-associated speck-like protein in P388D1 murine lymphoma cells affects metastatic properties. *Hematol Oncol*. 2012; 30(2):62–9. Epub 2011 Aug 3. doi: [10.1002/hon.1010](https://doi.org/10.1002/hon.1010) PMID: [21812013](https://pubmed.ncbi.nlm.nih.gov/21812013/)
16. Liu W, Luo Y, Dunn JH, Norris DA, Dinarello CA, Fujita M. Dual role of apoptosis-associated speck-like protein containing a CARD (ASC) in tumorigenesis of human melanoma. *J Invest Dermatol*. 2013; 133(2):518–27. Epub 2012 Aug 30. doi: [10.1038/jid.2012.317](https://doi.org/10.1038/jid.2012.317) PMID: [22931929](https://pubmed.ncbi.nlm.nih.gov/22931929/)
17. Liu Q, Jin J, Ying J, Cui Y, Sun M, Zhang L, et al. Epigenetic inactivation of the candidate tumor suppressor gene ASC/TMS1 in human renal cell carcinoma and its role as a potential therapeutic target. *Oncotarget*. 2015; 6(26):22706–23. doi: [10.18632/oncotarget.4256](https://doi.org/10.18632/oncotarget.4256) PMID: [26093088](https://pubmed.ncbi.nlm.nih.gov/26093088/)
18. Lloyd RV, Erickson LA, Jin L, Kulig E, Qian X, Chevillat JC, et al. p27kip1: a multifunctional cyclin-dependent kinase inhibitor with prognostic significance in human cancers. *Am J Pathol*. 1999; 154(2):313–23. Review. doi: [10.1016/S0002-9440\(10\)65277-7](https://doi.org/10.1016/S0002-9440(10)65277-7) PMID: [10027389](https://pubmed.ncbi.nlm.nih.gov/10027389/)
19. Bar J, Cohen-Noyman E, Geiger B, Oren M. Attenuation of the p53 response to DNA damage by high cell density. *Oncogene*. 2004; 23(12):2128–37. doi: [10.1038/sj.onc.1207325](https://doi.org/10.1038/sj.onc.1207325) PMID: [14755247](https://pubmed.ncbi.nlm.nih.gov/14755247/)
20. Perucca P, Cazzalini O, Madine M, Savio M, Laskey RA, Vannini V, et al. Loss of p21 CDKN1A impairs entry to quiescence and activates a DNA damage response in normal fibroblasts induced to quiescence. *Cell Cycle*. 2009; 8(1):105–14. Epub 2009 Jan 1. doi: [10.4161/cc.8.1.7507](https://doi.org/10.4161/cc.8.1.7507) PMID: [19106607](https://pubmed.ncbi.nlm.nih.gov/19106607/)
21. Becker SF, Mayor R, Kashef J. Cadherin-11 mediates contact inhibition of locomotion during *Xenopus* neural crest cell migration. *PLoS One*. 2013 Dec 31; 8(12): e 85717.
22. Leontieva OV, Demidenko ZN, Blagosklonny MV. Contact inhibition and high cell density deactivate the mammalian target of rapamycin pathway, thus suppressing the senescence program. *Proc Natl Acad Sci U S A*. 2014; 111(24):8832–7. Epub 2014 Jun 2. doi: [10.1073/pnas.1405723111](https://doi.org/10.1073/pnas.1405723111) PMID: [24889617](https://pubmed.ncbi.nlm.nih.gov/24889617/)
23. Kelsey L, Katoch P, Ray A, Mitra S, Chakraborty S, Lin MF, et al. Vitamin D3 regulates the formation and degradation of gap junctions in androgen-responsive human prostate cancer cells. *PLoS One*. 2014 Sep 4; 9(9): e106437. doi: [10.1371/journal.pone.0106437](https://doi.org/10.1371/journal.pone.0106437) PMID: [25188420](https://pubmed.ncbi.nlm.nih.gov/25188420/)
24. Kato H, Naiki-Ito A, Naiki T, Suzuki S, Yamashita Y, Sato S, et al. Connexin 32 dysfunction promotes ethanol-related hepatocarcinogenesis via activation of Dusp1-Erk axis. *Oncotarget*. 2016 Jan 12; 7(2):2009–21. doi: [10.18632/oncotarget.6511](https://doi.org/10.18632/oncotarget.6511) PMID: [26655499](https://pubmed.ncbi.nlm.nih.gov/26655499/)
25. Mariathasan S, Monack DM. Inflammasome adaptors and sensors: intracellular regulators of infection and inflammation. *Nat Rev Immunol*. 2007; 7(1):31–40. doi: [10.1038/nri1997](https://doi.org/10.1038/nri1997) PMID: [17186029](https://pubmed.ncbi.nlm.nih.gov/17186029/)
26. Datta R, Oki E, Endo K, Biedermann V, Ren J, Kufe D. XIAP regulates DNA damage-induced apoptosis downstream of caspase-9 cleavage. *J Biol Chem*. 2000; 275(41):31733–8. doi: [10.1074/jbc.M910231199](https://doi.org/10.1074/jbc.M910231199) PMID: [10930419](https://pubmed.ncbi.nlm.nih.gov/10930419/)
27. Ohtsuka T, Ryu H, Minamishima YA, Macip S, Sagara J, Nakayama KI, et al. ASC is a Bax adaptor and regulates the p53-Bax mitochondrial apoptosis pathway. *Nat Cell Biol*. 2004; 6(2):121–8. Epub 2004 Jan 18. doi: [10.1038/ncb1087](https://doi.org/10.1038/ncb1087) PMID: [14730312](https://pubmed.ncbi.nlm.nih.gov/14730312/)
28. Erl W, Hansson GK, de Martin R, Draude G, Weber KS, Weber C. Nuclear factor-kappa B regulates induction of apoptosis and inhibitor of apoptosis protein-1 expression in vascular smooth muscle cells. *Circ Res*. 1999; 84(6):668–77. PMID: [10189354](https://pubmed.ncbi.nlm.nih.gov/10189354/)
29. Ghebeh H, Al-Khalidi S, Olabi S, Al-Dhfyhan A, Al-Mohanna F, Barnawi R, et al. Fascin is involved in the chemotherapeutic resistance of breast cancer cells predominantly via the PI3K/Akt pathway. *Br J Cancer*. 2014; 111(8):1552–61. Epub 2014 Aug 12. doi: [10.1038/bjc.2014.453](https://doi.org/10.1038/bjc.2014.453) PMID: [25117814](https://pubmed.ncbi.nlm.nih.gov/25117814/)
30. Masumoto J, Dowds TA, Schaner P, Chen FF, Ogura Y, Li M, et al. ASC is an activating adaptor for NF-kappa B and caspase-8-dependent apoptosis. *Biochem Biophys Res Commun*. 2003; 303: 69–73. PMID: [12646168](https://pubmed.ncbi.nlm.nih.gov/12646168/)
31. Chung H, Vilaysane A, Lau A, Stahl M, Morampudi V, Bondzi-Simpson A, et al. NLRP3 regulates a non-canonical platform for caspase-8 activation during epithelial cell apoptosis. *Cell Death Differ*. 2016 Feb 19. Epub ahead of print
32. McConnell BB, Vertino PM. Activation of a caspase-9-mediated apoptotic pathway by subcellular redistribution of the novel caspase recruitment domain protein TMS1. *Cancer Res*. 2000; 60:6243–7. PMID: [11103777](https://pubmed.ncbi.nlm.nih.gov/11103777/)
33. Kavuri SM, Geserick P, Berg D, Dimitrova DP, Feoktistova M, Siegmund D, et al. Cellular FLICE-inhibitory protein (cFLIP) isoforms block CD95—and TRAIL death receptor-induced gene induction irrespective of processing of caspase-8 or cFLIP in the death-inducing signaling complex. *J Biol Chem*. 2011; 286(19):16631–46. Epub 2011 Mar 22. doi: [10.1074/jbc.M110.148585](https://doi.org/10.1074/jbc.M110.148585) PMID: [21454681](https://pubmed.ncbi.nlm.nih.gov/21454681/)

34. Dickens LS, Powley IR, Hughes MA, MacFarlane M. The 'complexities' of life and death receptor signaling platforms. *Exp Cell Res*. 2012; 318(11):1269–77. Epub 2012 Apr 17. Review. doi: [10.1016/j.yexcr.2012.04.005](https://doi.org/10.1016/j.yexcr.2012.04.005) PMID: [22542855](https://pubmed.ncbi.nlm.nih.gov/22542855/)
35. Cain K, Brown DG, Langlais C, Cohen GM. Caspase activation involves the formation of the aposome a large (approximately 700 kDa) caspase-activating complex. *J Biol Chem*. 1999; 274(32):22686–92. PMID: [10428850](https://pubmed.ncbi.nlm.nih.gov/10428850/)
36. Würstle ML, Rehm M. A systems biology analysis of apoptosome formation and apoptosis execution supports allosteric procaspase-9 activation. *J Biol Chem*. 2014; 289(38):26277–89. Epub 2014 Aug 8. doi: [10.1074/jbc.M114.590034](https://doi.org/10.1074/jbc.M114.590034) PMID: [25107908](https://pubmed.ncbi.nlm.nih.gov/25107908/)
37. de Rivero Vaccari JP, Lotocki G, Marcillo AE, Dietrich WD, Keane RW. A molecular platform in neurons regulates inflammation after spinal cord injury. *J Neurosci*. 2008; 28(13):3404–14. doi: [10.1523/JNEUROSCI.0157-08.2008](https://doi.org/10.1523/JNEUROSCI.0157-08.2008) PMID: [18367607](https://pubmed.ncbi.nlm.nih.gov/18367607/)
38. Ritt MG, Mayor J, Wojcieszyn J, Smith R, Barton CL, Modiano JF. Sustained nuclear localization of p21/WAF-1 upon growth arrest induced by contact inhibition. *Cancer Lett*. 2000; 158(1):73–84. PMID: [10940512](https://pubmed.ncbi.nlm.nih.gov/10940512/)
39. Larson DM, Wroblewski MJ, Sagar GD, Westphale EM, Beyer EC. Differential regulation of connexin43 and connexin37 in endothelial cells by cell density, growth, and TGF-beta 1. *Am J Physiol*. 1997; 272(2 Pt 1):C405–15. PMID: [9124282](https://pubmed.ncbi.nlm.nih.gov/9124282/)
40. Krutovskikh VA, Piccoli C, Yamasaki H. Gap junction intercellular communication propagates cell death in cancerous cells. *Oncogene*. 2002 Mar 27; 21(13):1989–99. Erratum in: *Oncogene* 2002 Jun 27;21(28):4471. doi: [10.1038/sj.onc.1205187](https://doi.org/10.1038/sj.onc.1205187) PMID: [11960371](https://pubmed.ncbi.nlm.nih.gov/11960371/)
41. Salat-Canela C, Sesé M, Peula C, Ramón y Cajal S, Aasen T. Internal translation of the connexin 43 transcript. *Cell Commun Signal*. 2014 May 8; 12:31. doi: [10.1186/1478-811X-12-31](https://doi.org/10.1186/1478-811X-12-31) PMID: [24884945](https://pubmed.ncbi.nlm.nih.gov/24884945/)